

Phase transition of an SU(3) symmetric spin-1 chain

Tohru Mashiko and Kiyohide Nomura

Department of Physics, Kyushu University, Fukuoka 819-0395, Japan

We investigate a phase transition in an SU(3) symmetric spin-1 chain. To study this transition, we numerically diagonalize an SU(3) symmetric Hamiltonian combining the Uimin-Lai-Sutherland (ULS) model Hamiltonian with the Hamiltonian of the exact trimer ground state (\mathbb{Z}_3 symmetry breaking). Our numerical results are discussed on the basis of the conformal field theory (CFT) and the renormalization group (RG). We then show the phase transition between a trimer liquid phase (massless, no long-range order) and a trimer phase (spontaneously \mathbb{Z}_3 symmetry breaking). Next, we find the central charge $c = 2$ in the massless phase, and $c < 2$ in the \mathbb{Z}_3 symmetry broken phase. From these results, we identify the universality class of the critical trimer liquid phase, as well as the phase boundary between these two phases.

1 Introduction

In condensed matter physics, phase transitions and critical phenomena are important subjects. In one- or two-dimensional quantum systems with continuous symmetry, quantum fluctuation is strong enough to prevent the long-range order, which makes critical phenomena complicated. As for the SU(3) symmetric spin-1 chains, there have been several studies investigating the critical phenomena and the universality class. It was found that the ground state is the critical trimer liquid (TL) state with no long-range order, in the cases of the Uimin-Lai-Sutherland (ULS) model [1–4] and the SU(3) symmetric Dimer-Trimer (DT) model [5, 6]. In general, critical phases of SU(ν) symmetric quantum spin chains (ν : integer) is stabilized by the \mathbb{Z}_ν symmetry [7, 8], the center of the SU(ν) group. In contrast, Hamiltonians describing the SU(3) trimer state were proposed [9–11], where there is a trimer long-range order and the \mathbb{Z}_3 symmetry is spontaneously broken. However, there remain unsolved problems with regard to the phase transition between the TL phase and the trimer phase. Therefore, it is necessary to study such phenomena in more detail. Revealing such phenomena gives basic theories to experiments and quantum simulations of ultracold alkaline earth metallic atoms in an optical lattice [12–14].

We here review an SU(3) symmetric spin-1 chain, the ULS model [1–4], to explain the critical phenomena of the TL. The ULS model is exactly solvable with the Bethe ansatz, and the ground state is the critical TL state. Affleck found [7, 8] that the universality class of the TL is the same as that of the level-1 SU(3) Wess-Zumino-Witten [SU(3)₁ WZW] model [15–17] with the central charge $c = 2$ and the scaling dimension $x = 2/3$ [18], by mapping the ULS model to the SU(3)₁ WZW model. Also, he found [7, 8] the quasi-long-range order and soft modes at the wave number $q = 0, \pm 2\pi/3$ in the TL state. Then, Itoi and Kato calculated [19] coefficients of logarithmic finite-size correction in the correlation functions in the case of the TL state. They also found [19] that the phase transition of the ULS model belongs to the Berezinskii-Kosterlitz-Thouless (BKT)-like universality class.

On the other hand, the pure trimer states, i.e., threefold degenerate states breaking translational invariance, were proposed [20, 21]. Here, the system follows periodic boundary conditions (PBCs). The pure trimer states on a spin-1 chain $|\psi_T\rangle$

are given as

$$|\psi_T\rangle = \begin{cases} \{\circ\circ\circ\}\{\circ\circ\circ\}\cdots\{\circ\circ\circ\}, \\ \circ\{\circ\circ\circ\}\cdots\{\circ\circ\circ\}\circ, \\ \circ\circ\{\circ\circ\circ\}\cdots\{\circ\circ\circ\}\circ, \end{cases} \quad (1)$$

where $\{\circ\circ\circ\}$ is the singlet state of the three adjacent spins (trimer). The state of the trimer is written as

$$\{\circ\circ\circ\} \equiv \frac{1}{\sqrt{6}} (|1, 0, -1\rangle + |0, -1, 1\rangle + |-1, 1, 0\rangle - |1, -1, 0\rangle - |0, 1, -1\rangle - |-1, 0, 1\rangle), \quad (2)$$

where 1, 0, -1 refers to a spin magnetic quantum number S^z . Several models with the pure trimer ground states were proposed [9–11], as a generalization of the Majumdar-Ghosh Hamiltonian [22] of the dimer ground state of the spin-1/2 chain. Also, there is a gap [11] between threefold degenerate ground state energy and eightfold degenerate elementary excitation spectrum.

In this paper, we numerically diagonalize the Hamiltonian combining the ULS Hamiltonian [1–4] \hat{H}_{ULS} with the trimer Hamiltonian [11] \hat{H}_{trimer} under PBCs to investigate the phase transition between the TL phase and the trimer phase. In Sec. 2, we define this Hamiltonian, which is composed only of exchange operators \hat{P}_{ij} . Numerical results of dispersion curves are shown in Sec. 3. In Sec. 4, we confirm that the phase transition is caused by a marginal operator [19], and then specify the universality class of the critical phenomena. Conclusion and discussion are shown in Sec. 5, where we discuss correlation functions describing the critical state of the TL and the long-range order of the trimer phase.

2 MODEL

To investigate the phase transition between the TL phase and the trimer phase, we numerically diagonalize the Hamiltonian defined as

$$\hat{H} \equiv \cos \phi \hat{H}_{\text{ULS}} + \sin \phi \hat{H}_{\text{trimer}}, \quad (3)$$

where the parameter ϕ is in the range of $0 \leq \phi \leq \pi/2$, and \hat{H}_{ULS} and \hat{H}_{trimer} will be defined in the next paragraph or later. In this section, we represent the Hamiltonian Eq. (3)

with the exchange operator $\hat{P}_{ii'}$, which swaps spins at site i with that at site i' , defined as

$$\hat{P}_{ii'}|\cdots S_i^z \cdots S_{i'}^z \cdots\rangle = |\cdots S_{i'}^z \cdots S_i^z \cdots\rangle, \quad (4)$$

where $|\cdots\rangle$ is a state vector of a spin system and S_i^z is a spin magnetic quantum number at site i .

First of all, we represent the ULS Hamiltonian with the exchange operator. The Hamiltonian of the ULS model is defined [1–4] as

$$\hat{H}_{\text{ULS}} \equiv \sum_{i=1}^N \left[(\hat{\mathbf{S}}_i \cdot \hat{\mathbf{S}}_j) + (\hat{\mathbf{S}}_i \cdot \hat{\mathbf{S}}_j)^2 \right], \quad (5)$$

where $\hat{\mathbf{S}}_i$ is a spin-1 operator at site i , and we define $j \equiv i + 1$. Also, there is the relation [3] $(\hat{\mathbf{S}}_i \cdot \hat{\mathbf{S}}_{i'}) + (\hat{\mathbf{S}}_i \cdot \hat{\mathbf{S}}_{i'})^2 = \hat{P}_{ii'} + \hat{1}$, where $\hat{1}$ is the identity operator. Therefore, the ULS Hamiltonian can be rewritten [3] as

$$\hat{H}_{\text{ULS}} = \sum_{i=1}^N \hat{P}_{ij}, \quad (6)$$

where we neglect a trivial constant.

Secondly, we introduce the trimer Hamiltonian based on the paper of Greiter and Rachel [11]. Here, we denote $\hat{c}_{i\sigma}^\dagger$ ($\hat{c}_{i\sigma}$) to be an operator which creates (annihilates) a spin-1 with $S^z = \sigma$ at site i , and define the SU(3) generators at site i as

$$\hat{J}_i^a \equiv \frac{1}{2} \sum_{\sigma, \sigma'=1,0,-1} \hat{c}_{i\sigma}^\dagger \lambda_{\sigma\sigma'}^a \hat{c}_{i\sigma'}, \quad a = 1, \dots, 8 \quad (7)$$

$$\hat{\mathbf{J}}_i \equiv \left(\hat{J}_i^1, \hat{J}_i^2, \hat{J}_i^3, \hat{J}_i^4, \hat{J}_i^5, \hat{J}_i^6, \hat{J}_i^7, \hat{J}_i^8 \right)^T, \quad (8)$$

where the λ^a are the Gell-Mann matrices (see Appendix A.1). The operators Eq. (7) satisfy the commutation relations

$$[\hat{J}_i^a, \hat{J}_{i'}^b] = \delta_{ii'} f^{abc} \hat{J}_i^c, \quad a, b, c = 1, \dots, 8 \quad (9)$$

where f^{abc} are the structure constants of SU(3) (see Appendix A.1), and we use the Einstein summation convention. Then, we define $\hat{\mathbf{J}}_i^{(\nu)}$ with an integer ν for neighboring sites $i, \dots, i + \nu - 1$ as,

$$\hat{\mathbf{J}}_i^{(\nu)} \equiv \sum_{i'=i}^{i+\nu-1} \hat{\mathbf{J}}_{i'}. \quad (10)$$

For the trimer states Eq. (2) on the four neighboring sites, the situation simplifies as we only have the two possibilities

$$\begin{cases} \{\circ \circ \circ\} \circ, \\ \{\circ \circ\} \{\circ \circ\}. \end{cases} \quad (11)$$

Here, $\{\circ \circ\}$ is the triplet state of the two adjacent spins, whose state vectors are given by

$$\{\circ \circ\} = \begin{cases} \frac{1}{\sqrt{2}}(|1, 0\rangle - |0, 1\rangle), \\ \frac{1}{\sqrt{2}}(|1, -1\rangle - |-1, 1\rangle), \\ \frac{1}{\sqrt{2}}(|0, -1\rangle - |-1, 0\rangle). \end{cases} \quad (12)$$

Note that Eqs. (11) and (12) are expressed [11] by the representations of SU(3) (see Appendix A.2). The quadratic Casimir

operator for these two representations Eq. (11) has eigenvalues [11] of $4/3$ and $10/3$ respectively. Therefore, the auxiliary operators can be written as [11]

$$\hat{H}_i = \left[\left(\hat{\mathbf{J}}_i^{(4)} \right)^2 - \frac{4}{3} \right] \left[\left(\hat{\mathbf{J}}_i^{(4)} \right)^2 - \frac{10}{3} \right]. \quad (13)$$

The trimer Hamiltonian is defined as

$$\hat{H}_{\text{trimer}} \equiv \sum_{i=1}^N \hat{H}_i. \quad (14)$$

Moreover, using the exchange operator $\hat{P}_{ii'}$, there is an equation [11] on the SU(3) generators as

$$\hat{\mathbf{J}}_i \hat{\mathbf{J}}_{i'} = \begin{cases} \frac{4}{3}, & (i = i') \\ \frac{1}{2} \left(\hat{P}_{ii'} - \frac{1}{3} \right). & (i \neq i') \end{cases} \quad (15)$$

Using Eqs. (13) – (15), the trimer Hamiltonian can be rewritten as

$$\begin{aligned} \hat{H}_{\text{trimer}} = \sum_{i=1}^N & \left[\hat{P}_{ij} + \frac{2}{3} \hat{P}_{ik} + \frac{1}{3} \hat{P}_{il} + \hat{P}_{ij} \hat{P}_{ik} + \hat{P}_{ik} \hat{P}_{ij} \right. \\ & + \frac{1}{2} \left(\hat{P}_{ij} \hat{P}_{il} + \hat{P}_{il} \hat{P}_{ij} + \hat{P}_{ik} \hat{P}_{il} + \hat{P}_{il} \hat{P}_{ik} \right) \\ & \left. + \frac{1}{3} \left(\hat{P}_{ij} \hat{P}_{kl} + \hat{P}_{ik} \hat{P}_{jl} + \hat{P}_{il} \hat{P}_{jk} \right) \right], \quad (16) \end{aligned}$$

where we define $k \equiv i + 2$, $l \equiv i + 3$.

From Eqs. (6) and (16), the Hamiltonian Eq. (3) is composed only of the exchange operators, which conserves the number of spins, N_1 , N_0 , N_{-1} for each state $S^z = 1, 0, -1$ respectively. Then, the full Hilbert space with 3^N dimensions is reduced to a subspace with $\frac{N!}{N_1!N_0!N_{-1}!}$ dimensions, ($N = N_1 + N_0 + N_{-1}$).

3 Dispersion curves

In this section, we show our numerical results of the dispersion curves of the model Eq. (3). Here, we make use of the conservation of the number of each spin mentioned in Sec. 2 and the translational symmetry for our numerical calculations.

Firstly, we let \hat{O}_t denote a translational operator, which shifts all spins in the system by one site. \hat{O}_t has an eigenvalue written as

$$\hat{O}_t |\cdots\rangle = e^{iq} |\cdots\rangle, \quad (17)$$

where q is the wave number. Under PBCs, $(\hat{O}_t)^N$ is an identity operator. The wave number thus should be $q = 2\pi n/N$ (n : integer).

The energy eigenvalue E is dependent on the wave number q and the total spin quantum number of the system S_T . Therefore, we let $E_{S_T}(q)$ be the lowest energy at q and S_T . We define the difference between $E_{S_T}(q)$ and the ground-state energy E_g as

$$\Delta E_{S_T}(q) \equiv E_{S_T}(q) - E_g. \quad (18)$$

Also, we let $E(q)$ denote the lowest energy at q and define the difference between $E(q)$ and E_g as

$$\Delta E(q) \equiv E(q) - E_g. \quad (19)$$

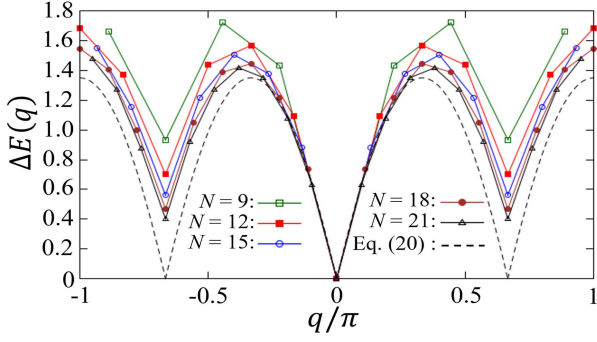


FIG. 1: Dispersion curves $\Delta E(q)$ in the case of $\phi = 0$ with $N = 9$ –21. The dashed line is a curve obtained using Eq. (20).

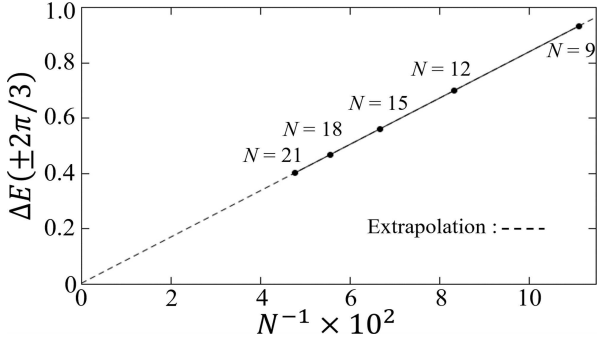


FIG. 2: Elementary excitation energy $\Delta E(\pm 2\pi/3)$ in the case of $\phi = 0$ as a function of N^{-1} .

3.1 Dispersion curves in the case of the ULS model ($\phi = 0$)

Figure 1 shows dispersion curves $\Delta E(q)$ with $N = 9$ –21 in the case of $\phi = 0$. The ground-state energy is the lowest energy at $q = 0$ and $S_T = 0$, that is, $E_g = E(0) = E_0(0)$. Also, there are soft modes at $q = 0, \pm 2\pi/3$ for all system sizes, as shown in Fig. 1. These results are consistent with the theory of Sutherland [3]. In this theory, $\Delta E(q)$ is given by

$$\Delta E(q) = D \left[\cos\left(\frac{\pi}{3} - |q|\right) - \frac{1}{2} \right], \quad \left(0 \leq |q| \leq \frac{2\pi}{3}\right)$$

$$\Delta E(q) = \Delta E\left(|q| - \frac{2\pi}{3}\right), \quad \left(\frac{2\pi}{3} \leq |q| \leq \pi\right)$$
(20)

in the thermodynamical limit, $N \rightarrow \infty$. Here, D is a non-universal constant. A dispersion curve gained from Eq. (20) is also given in Fig. 1. Furthermore, we reveal that $E(\pm 2\pi/3) = E_1(\pm 2\pi/3) = E_2(\pm 2\pi/3)$, namely, an eightfold degeneracy. Considering the fact that soft modes appear at $q = 0, \pm 2\pi/3$, one should carry out numerical calculations only in cases where N is a multiple of 3 in later sections as well.

Figure 2 illustrates $\Delta E(\pm 2\pi/3)$ replotted for $N = 9$ –21. The elementary excitation energy $\Delta E(\pm 2\pi/3)$ depends linearly on N^{-1} . We extrapolate $\Delta E(\pm 2\pi/3)$ with the function $\Delta E(\pm 2\pi/3) = a_0 + a_1 N^{-1}$, where a_0 and a_1 are constants. We then obtain $a_0 = 0.0045 \pm 0.0001$, and thus, it seems that the system is massless.

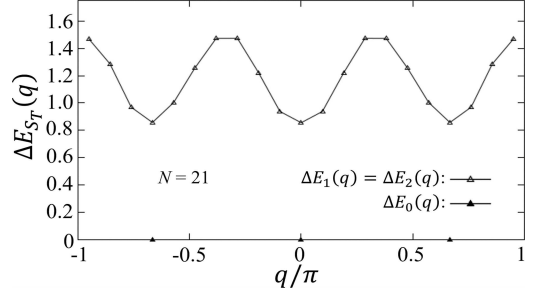
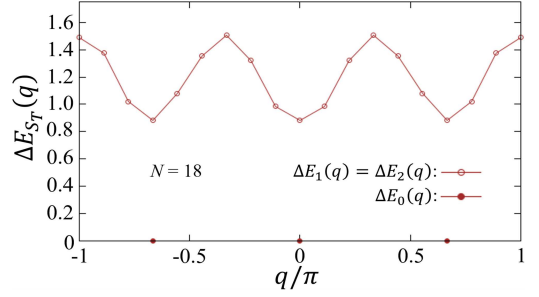


FIG. 3: Dispersion curves $\Delta E_{S_T}(q)$ in the case of $\phi = \pi/2$ with $N = 15$ –21.

3.2 Dispersion curves in the case of the trimer model ($\phi = \pi/2$)

Figure 3 shows dispersion curves $\Delta E_{S_T}(q)$ with $N = 15$ –21 in the case of $\phi = \pi/2$. We find that the ground-state energy is threefold degenerated, $E_g = E_0(0) = E_0(\pm 2\pi/3)$. We also find a gap between the E_g and the eightfold degenerated elementary excitation spectrum, $\Delta E_1(q) = \Delta E_2(q)$. According to Greiter and Rachel [11], elementary excitations are realized by the domain wall $\{\circ\circ\}$, that is

$$\dots \{\circ\circ\}\{\circ\circ\}\{\circ\circ\}\dots \quad (21)$$

If $N < 15$, the domain wall appear only in the case of $N = 3n - 1$ (n : integer). On the other hand, if $N \geq 15$, the domain wall can appear in the case of $N = 3n$ as well, for example

$$\{\circ\circ\}\{\circ\circ\}\{\circ\circ\}\{\circ\circ\}\{\circ\circ\}\{\circ\circ\}, \quad (N = 15) \quad (22)$$

under PBCs. Therefore, we believe that the excitations shown in Fig. 3 is realized by the domain wall $\{\circ\circ\}$. Moreover, the gap seems not to depend on the system size N , which is consistent with the paper of Greiter and Rachel [11].

3.3 spin wave velocity

We calculate the spin wave velocity, which we utilize for later calculations of the central charge. Note that the spin wave velocity and the central charge are valid only in the case of the massless TL phase. The spin wave velocity v_0 is defined as

$$v_0 \equiv \left. \frac{dE(q)}{dq} \right|_{q=0}. \quad (23)$$

The velocity is a function of N , $v_0(N)$. In our numerical calculations, we investigate the slope of the dispersion curves to obtain $v_0(N)$ written as

$$v_0(N) = \frac{E(2\pi/N) - E(0)}{2\pi/N}. \quad (24)$$

The spin wave velocity is plotted in Fig. 4. The area in the left side of Fig. 4, where size N dependency of $v_0(N)$ is small, seems to be the TL phase, which we discuss in more detail in 3 the next section.

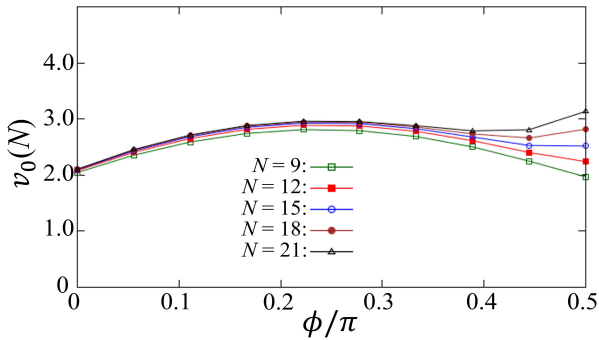


FIG. 4: Spin wave velocity $v_0(N)$ as a function of ϕ with $N = 9-21$.

4 Phase transition and critical phenomena

In this section, we investigate the phase transition between the TL phase and the trimer phase, which is caused by a marginal operator [19]. We then calculate a critical exponent, the central charge c , to specify the universality class of the system. Here, we define the difference between $E_0(q)$ and $E_2(q)$ as

$$\Delta E_{\text{so}}(q) \equiv E_0(q) - E_2(q). \quad (25)$$

4.1 Renormalization discussion on the $SU(3)_1$ WZW model

In this subsection, we investigate the phase transition characterized by \mathbb{Z}_3 symmetry breaking on the basis of the RG [19].

4.1.1 phase transition

In Fig. 5, we plot $N\Delta E_{\text{so}}(\pm 2\pi/3)$, for various ϕ with $N = 9-21$. As shown in Fig. 5, we firstly find that the value of $N\Delta E_{\text{so}}(\pm 2\pi/3)$ changes from positive to negative at a certain point ϕ_c for all system sizes. One can see that the size dependence of the crossing points $\phi_c(N)$ is very small, and that the slopes near $\phi_c(N)$ are almost the same. On the contrary, there is relatively large size dependence far from $\phi_c(N)$. We discuss these numerical results on the basis of the theory of Itoi and Kato [19]. They analytically studied the action of the field in the vicinity of the system described by the $SU(3)_1$ WZW model, and then derived renormalization-group equations of the action. By solving the renormalization-group equations, they found [19] that if the system is massless, $\Delta E_{\text{so}}(\pm 2\pi/3)$

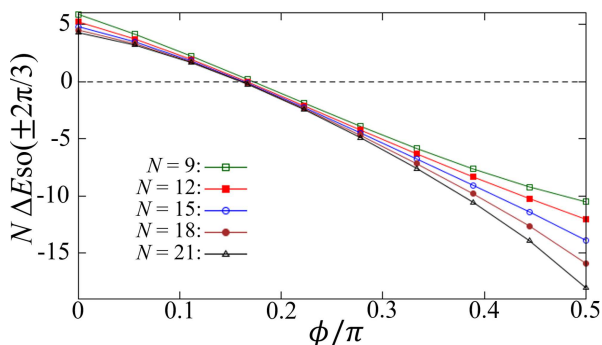


FIG. 5: $N\Delta E_{\text{so}}(\pm 2\pi/3)$ as a function of ϕ with $N = 9-21$.

satisfies the relation

$$\Delta E_{\text{so}}\left(\pm \frac{2\pi}{3}\right) > 0. \quad (26)$$

They also found [19] that if the system is \mathbb{Z}_3 ordered, $\Delta E_{\text{so}}(\pm 2\pi/3)$ satisfies the relation

$$\Delta E_{\text{so}}\left(\pm \frac{2\pi}{3}\right) < 0. \quad (27)$$

By comparing our numerical results in Fig. 5 with the theory [19], we find that the region $\phi < \phi_c$ is the \mathbb{Z}_3 symmetric (massless) phase, and the region $\phi > \phi_c$ is the \mathbb{Z}_3 ordered phase. In other words, there occurs a phase transition at $\phi = \phi_c$.

4.1.2 phase transition and the renormalization group

The phase transition shown in Fig. 5 is described by the renormalization-group equation [19] of the scaling variable g_1 for the marginal operator, Eq. (71), (see Appendix B). The solution of Eq. (71) is

$$g_1(l) = g_1(0) \left(1 - \frac{3}{2\sqrt{2}}g_1(0)l\right)^{-1}, \quad (28)$$

where $l \equiv \ln N$. Here, $g_1(0) = 0$ is a fixed point, which corresponds to the phase boundary ϕ_c . Also, in the vicinity of the fixed point, it is expected [19, 23, 24] to be

$$g_1(0) = C(\phi - \phi_c), \quad (29)$$

where C is a non-universal constant of proportionality. We will discuss the expectation Eq. (29) in more detail in Sec 4.2.2. In the case of $g_1(0) < 0$, $g_1(l)$ converges zero as $l \rightarrow \infty$ (marginally irrelevant), which means that the region $g_1(0) < 0$ corresponds to the massless phase $\phi < \phi_c$. In the case of $g_1(0) > 0$, $g_1(l)$ diverges (marginally relevant), which means that the region $g_1(0) > 0$ corresponds to the \mathbb{Z}_3 ordered phase $\phi > \phi_c$. Now let us choose to halt the renormalization at the point where $g_1(l) = O(1)$ in the massive region.

Considering the marginal operator, the excitation energy $\Delta E_{S_T}(\pm 2\pi/3)$ is written [19, 23, 24] as

$$\Delta E_{S_T}\left(\pm \frac{2\pi}{3}\right) = \frac{2\pi v_0}{N} \left(\frac{2}{3} + d_{S_T}g_1(l)\right), \quad (30)$$

where d_{S_T} is a coefficient depending on S_T with the values [7, 8, 19] of

$$d_0 = -\frac{4}{3\sqrt{2}}, \quad d_1 = d_2 = \frac{1}{6\sqrt{2}}. \quad (31)$$

Therefore, from Eqs. (25) and (30), we obtain

$$N\Delta E_{\text{so}}\left(\pm \frac{2\pi}{3}\right) = -\frac{3\pi}{\sqrt{2}}v_0(N)g_1(l). \quad (32)$$

4.1.3 massless phase

As shown in Fig. 5, in the massless phase ($g_1(0) < 0$) near $\phi = 0$, $N\Delta E_{\text{so}}(\pm 2\pi/3)$ gets smaller depending on N . We discuss this fact on the basis of the renormalization group [19, 23].

In the massless phase near $\phi = 0$, the limit of $g_1(0) \ll -1$, Eq. (28) can be approximated as

$$g_1(l) \approx -\frac{2\sqrt{2}}{3} \cdot \frac{1}{\ln N}, \quad (33)$$

in the SU(3) symmetric critical system. From Eqs. (32) and (33), we obtain

$$N\Delta E_{\text{so}}\left(\pm\frac{2\pi}{3}\right)\approx\frac{2\pi v_0(N)}{\ln N}. \quad (34)$$

Therefore, $N\Delta E_{\text{so}}(\pm 2\pi/3)$ in Fig. 5 becomes smaller proportional to $1/\ln N$, since $v_0(N)$ is not very dependent on N as shown in Fig. 4.

4.1.4 \mathbb{Z}_3 ordered phase

In the \mathbb{Z}_3 ordered phase ($g_1(0) > 0$), $N\Delta E_{\text{so}}(\pm 2\pi/3)$ negatively increases depending on N in the vicinity of $\phi = \pi/2$, as shown in Fig. 5. This fact can also be discussed on the basis of the renormalization group [19,23]. If $g_1(0) > 0$, $g_1(l)$ monotonically increases depending on l , as shown in Eq. (28). Therefore, Eq.(32) shows that $N\Delta E_{\text{so}}(\pm 2\pi/3)$ negatively increases as N increases. This means that in the thermodynamical limit, $E_0(\pm 2\pi/3)$ degenerate with the ground state energy E_g , which corresponds to the \mathbb{Z}_3 symmetry breaking (the trimer state).

Next, we discuss the correlation length in the \mathbb{Z}_3 ordered phase. Here, we put $g_1(l') = 1$, where l' is the value of l when the scaling variable is sufficiently renormalized. Substituting $g_1(l') = 1$ for Eq. (28), we obtain

$$g_1(0) = \left(1 + \frac{3}{2\sqrt{2}}l'\right)^{-1}. \quad (35)$$

Also, because of $\xi \sim e^{l'}$, the correlation length can be written

$$\xi \sim \exp\left(\frac{2\sqrt{2}}{3}\frac{1-g_1(0)}{g_1(0)}\right). \quad (36)$$

If $g_1(0) \rightarrow 0$, we obtain

$$\xi \sim \exp\left(\frac{2\sqrt{2}}{3}\frac{1}{g_1(0)}\right). \quad (37)$$

In other words, the correlation length diverges as ϕ approaches the transition point, and the function form resembles that of the BKT-like [19].

4.2 Renormalization discussion in the vicinity of $\phi = \phi_c$

In this subsection, we discuss the region in the vicinity of ϕ_c . Figure 6 shows a close-up of Fig. 5 around the phase boundary ϕ_c . Here, we let ϕ_{c+} and ϕ_{c-} denote parameters ϕ in the vicinity of ϕ_c in the region $\phi > \phi_c$ and $\phi < \phi_c$ respectively.

4.2.1 phase boundary

From the results in Fig 6, we calculate the phase boundary ϕ_c for each system size utilizing the equation

$$\frac{N\Delta E_{\text{so}}(\pm 2\pi/3)|_{\phi=\phi_{c+}}}{\phi_{c+} - \phi_c} = \frac{N\Delta E_{\text{so}}(\pm 2\pi/3)|_{\phi=\phi_{c-}}}{\phi_{c-} - \phi_c}, \quad (38)$$

where Eq. (38) is reliable because $\Delta E_{\text{so}}(\pm 2\pi/3)$ depends linearly on $\phi - \phi_c$ in the vicinity of ϕ_c . We plot $\phi_c(N)$ in Fig. 7. The correction terms $O(N^{-2})$ in Fig. 7 can be explained by descendant fields of the identity operator with the scaling dimension $x = 4$ [24–27]. Therefore, $\phi_c(N)$ behaves as

$$\phi_c(N) = \phi_c + A_1 N^{-2} + A_2 N^{-4} + O(N^{-6}), \quad (39)$$

where A_1 and A_2 are non-universal constants. Fitting the data with a function $\phi_c(N) = \phi_c + A_1 N^{-2} + A_2 N^{-4}$, we obtain

$$\frac{\phi_c}{\pi} = 0.157794 \pm 0.000001, \quad (40)$$

when we extrapolate $\phi_c(N)$ with $N = 9-21$. Therefore, we put $\phi_c = 0.15779\pi$ later.

4.2.2 renormalization group and the slope of $N\Delta E_{\text{so}}(\pm 2\pi/3)$ in the vicinity of $\phi = \phi_c$

In Fig. 5, in the vicinity of ϕ_c , $N\Delta E_{\text{so}}(\pm 2\pi/3)$ seems almost independent of N . We discuss this fact on the basis of the theory of Itoi and Kato [19].

For $|g_1(0)| \ll 1$, Eq. (28) can be approximated as

$$g_1(l) \approx g_1(0). \quad (41)$$

Therefore, substituting Eq. (41) for Eq. (32), we obtain

$$N\Delta E_{\text{so}}\left(\pm\frac{2\pi}{3}\right)\approx-\frac{3\pi}{\sqrt{2}}v_0(N)g_1(0), \quad (42)$$

From Eq. (42), the behavior of Fig. 5 in the vicinity of ϕ_c are explained. Also, we confirm the expectation Eq. (29).

Next, we derive the constant C in Eq. (29). To begin with, utilizing Eqs. (29) and (42), we obtain a relation

$$\begin{aligned} N \left[\Delta E_{\text{so}}\left(\pm\frac{2\pi}{3}\right)\Big|_{\phi=\phi_{c+}} - \Delta E_{\text{so}}\left(\pm\frac{2\pi}{3}\right)\Big|_{\phi=\phi_{c-}} \right] \\ \approx -\frac{3\pi C}{\sqrt{2}} \left[(\phi_{c+} - \phi_c)v_0(N)\Big|_{\phi=\phi_{c+}} - (\phi_{c-} - \phi_c)v_0(N)\Big|_{\phi=\phi_{c-}} \right] \\ \approx -\frac{3\pi C}{\sqrt{2}} v_{\text{av}}(N)(\phi_{c+} - \phi_{c-}), \end{aligned} \quad (43)$$

$$v_{\text{av}}(N) \equiv \frac{v_0(N)\Big|_{\phi=\phi_{c+}} + v_0(N)\Big|_{\phi=\phi_{c-}}}{2}. \quad (44)$$

We plot the slope of $N\Delta E_{\text{so}}(\pm 2\pi/3)$ defined as

$$\begin{aligned} f(N) \equiv \\ \frac{N \left[\Delta E_{\text{so}}(\pm 2\pi/3)\Big|_{\phi=\phi_{c+}} - \Delta E_{\text{so}}(\pm 2\pi/3)\Big|_{\phi=\phi_{c-}} \right]}{\phi_{c+} - \phi_{c-}}, \end{aligned} \quad (45)$$

in Fig. 8 as a function of N^{-2} . From Eqs. (43) and (45), the constant C can be written

$$C \approx -\frac{\sqrt{2}}{3\pi} \cdot \frac{f(N)}{v_{\text{av}}(N)} = -\frac{\sqrt{2}}{3\pi} \cdot \frac{f(\infty)}{v_{\text{av}}(\infty)}. \quad (46)$$

We then calculate $f(\infty)$ and $v_{\text{av}}(\infty)$ with Figs. 4 and 8, and the functions [24–27]

$$f(N) = f(\infty) + B_1 N^{-2} + B_2 N^{-4} + O(N^{-6}), \quad (47)$$

$$v_{\text{av}}(N) = v_{\text{av}}(\infty) + B'_1 N^{-2} + B'_2 N^{-4} + O(N^{-6}), \quad (48)$$

where $B_1, B_2, B'_1,$ and B'_2 are non-universal constants. Fitting the data with functions $f(N) = f(\infty) + B_1 N^{-2} + B_2 N^{-4}$ and $v_{\text{av}}(N) = v_{\text{av}}(\infty) + B'_1 N^{-2} + B'_2 N^{-4}$, we obtain

$$f(\infty) = -11.5566 \pm 0.0001, \quad (49)$$

$$v_{\text{av}}(\infty) = 2.89986 \pm 0.00002, \quad (50)$$

when we extrapolate them with $N = 9-21$. By substituting Eqs. (49) and (50) for Eq. (46), we obtain $C \approx 0.59797$.

4.3 Central charge

Here, we calculate the central charge c , which characterizes the quantum anomaly and specifies the universality class. In the critical state of one-dimensional quantum systems under PBCs, the ground-state energy density at N follows [28, 29] the equation

$$\frac{E_g(N)}{N} = \epsilon_\infty - \frac{\pi v_0 c}{6N^2}, \quad (51)$$

where ϵ_∞ is the ground-state energy density in the case of $N \rightarrow \infty$. Note that the central charge has a logarithmic finite-size correction [19, 23] with the form of $\frac{4}{9}(\ln N)^{-3}$. From Eq. (34), we estimate $(\ln N)^{-1} \approx 0.32$ in the cases of $N = 21$ and $\phi \approx 0$, and thus $\frac{4}{9}(\ln N)^{-3} \approx 0.014$, which is small enough compared to $c = 2$. Therefore, we neglect the logarithmic correction in the central charge. In Eq. (51), one can numerically calculate E_g and v_0 , but there remain two constants, ϵ_∞ and c , as unknown values. By removing the constant term ϵ_∞ in Eq. (51), we thus calculate the effective central charge $c(N)$ as

$$\begin{aligned} \frac{E_g(N)}{N} - \frac{E_g(N-3)}{N-3} \\ = -\frac{\pi}{6} \left[\frac{v_0(N)}{N^2} - \frac{v_0(N-3)}{(N-3)^2} \right] c(N). \end{aligned} \quad (52)$$

Figure 9 shows the effective central charge as a function of ϕ for different system sizes, $N = 12-21$. The effective central charge was firstly numerically calculated in the case of the CFT with $c = 1$ [30]. In this article, we investigate the effective central charge utilizing Eq. (52). Equation (51) is true only in the case of the massless phase certainly, but we can apply Eq. (52) even to systems in a massive phase as well. We find that the effective central charges smoothly converge to $c = 2$ as $N \rightarrow \infty$ in the region $\phi < \phi_c$ (Fig. 10). In Fig. 10, similarly to Eq. (39), we extrapolate the effective central charge $c(N)$ as [24–27]

$$c(N) = c + C_1(N-3/2)^{-2} + C_2(N-3/2)^{-4} + O((N-3/2)^{-6}), \quad (53)$$

where C_1 and C_2 are constants. Then, we obtain $c = 1.97963 \pm 0.00006$ when we extrapolate the $c(N)$ with the function Eq. (53) with $N = 12-21$.

On the other hand, in the region $\phi > \phi_c$, the effective central charge shows a decline as ϕ approaches $\pi/2$. Moreover, around $\phi = \phi_c$, there are no sharp decline of $c(N)$ because of the logarithmic correction [23] $O((\ln N)^{-3})$.

Comparing our numerical results in Figs. 9 and 10 with Zamolodchikov's c -theorem [31] and the theory of Itoi and Kato [19], we find that the region $\phi < \phi_c$ is illustrated by the CFT with $c = 2$ (critical phase), whereas the region $\phi > \phi_c$ is a massive phase.

4.4 Scaling dimension

In this subsection, we calculate the scaling dimension x , which is one of the critical exponents, at the boundary ($\phi = \phi_c$). Here, we rewrite elementary excitation energy at a certain S_T , Eq. (30), as

$$\Delta E_{S_T} \left(\pm \frac{2\pi}{3} \right) = \frac{2\pi v_0}{N} [x + d_{S_T} g_1(l)], \quad (54)$$

where we put $0 < g_1(l) \ll 1$. We derive the scaling dimension x by removing $d_{S_T} g_1(l)$ in Eq. (54) from the values in Eq. (31)

as

$$\begin{aligned} \frac{1}{9} \left[\Delta E_0 \left(\pm \frac{2\pi}{3} \right) + 3\Delta E_1 \left(\pm \frac{2\pi}{3} \right) + 5\Delta E_2 \left(\pm \frac{2\pi}{3} \right) \right] \\ = \frac{2\pi v_0(N)}{N} x(N). \end{aligned} \quad (55)$$

Similarly to Eq. (39), the effective scaling dimension $x(N)$ behaves as [24–27]

$$x(N) = x + D_1 N^{-2} + D_2 N^{-4} + O(N^{-6}), \quad (56)$$

where D_1 and D_2 are constants.

Figure 11 shows the effective scaling dimension $x(N)$ at $\phi = \phi_c$. We obtain $x = 0.666616 \pm 0.000004$ when we extrapolate the $x(N)$ with the function Eq. (56) in the cases of $N = 9-21$.

These numerical results at $\phi = \phi_c$ point are in line with the scaling dimension $x = 2/3$ of the $SU(3)_1$ WZW model [15–17].

5 CONCLUSION AND DISCUSSION

We have investigated the model Eq. (3) to clarify the critical behavior when changing the parameter ϕ . First of all, we find that soft modes appear at the wave number $q = 0, \pm 2\pi/3$ in both cases of $\phi = 0$ and $\phi = \pi/2$. Secondly, we find that the phase transition is caused by a marginal operator. In other words, there occurs a phase transition between the massless (marginally irrelevant) phase and the \mathbb{Z}_3 symmetry broken (marginally relevant) phase at $\phi_c = 0.15779\pi$. In the case of $SU(\nu)$ symmetric systems, where the critical phenomena are caused by the marginal operator, there are only a few numerical researches [30, 32, 33] combining renormalization group discussion. Thirdly, by investigating the central charge and the scaling dimension, we find that the region $\phi < \phi_c$ is a critical phase with $c = 2$ and $x = 2/3$ whereas the region $\phi > \phi_c$ is a massive phase. From these numerical results, we conclude that there occurs a phase transition at $\phi = \phi_c$ between the TL phase ($\phi < \phi_c$) and the trimer phase ($\phi > \phi_c$).

Here, we discuss several correlation functions in the $SU(3)$ symmetric TL phase to discuss the critical behavior. First of all, we discuss the spin correlation function and the spin-quadrupolar correlation function, which correspond to the energy of the triplet state $\Delta E_1(\pm 2\pi/3)$ and the quintuplet state $\Delta E_2(\pm 2\pi/3)$ respectively. It is expected [19, 34, 35] to be

$$\begin{aligned} \langle \hat{S}_i \cdot \hat{S}_{i+r} \rangle &= \langle \hat{Q}_{(i)}^{\mu\nu} \hat{Q}_{(i+r)\mu\nu} \rangle \\ &\propto \cos \left(\frac{2\pi}{3} r \right) r^{-4/3} (\ln r)^{2/9}, \end{aligned} \quad (57)$$

$$\hat{Q}_{(i)}^{\mu\nu} \equiv \frac{1}{2} \left\{ \hat{S}_i^\mu, \hat{S}_i^\nu \right\} - \frac{2}{3} \delta^{\mu\nu}, \quad (58)$$

from $c = 2$ and $x = 2/3$. Here, $\hat{Q}_{(i)}^{\mu\nu}$ is the spin-quadrupolar order parameter at site i , which is symmetric and traceless. Secondly, Schmitt et al. proposed [9] an order parameter corresponding to the singlet state $\Delta E_0(\pm 2\pi/3)$, which is defined as

$$\hat{T}_i \equiv \hat{T}_i^P - \langle \hat{T}_i^P \rangle, \quad \hat{T}_i^P \equiv |\{i, j, k\}\rangle \langle \{i, j, k\}|, \quad (59)$$

where the state vector of $|\{i, j, k\}\rangle$ is the same as $\{\circ \circ \circ\}$, Eq. (2), and we put $j \equiv i + 1$ and $k \equiv i + 2$. The correlation function of \hat{T}_i is expected [19] to be

$$\langle \hat{T}_i \hat{T}_{i+r} \rangle \propto \cos \left(\frac{2\pi}{3} r \right) r^{-4/3} (\ln r)^{-16/9}. \quad (60)$$

In the \mathbb{Z}_3 ordered phase, the correlation functions behave as follows. As for the spin correlation function and the spin-quadrupolar correlation function, it is expected to be

$$\langle \hat{\mathbf{S}}_i \cdot \hat{\mathbf{S}}_{i+r} \rangle = \langle \hat{Q}_{(i)}^{\mu\nu} \hat{Q}_{(i+r)\mu\nu} \rangle \propto \cos\left(\frac{2\pi}{3}r\right) e^{-r/\xi}, \quad (61)$$

where the correlation length ξ is defined in Eq. (36). Next, the correlation function of Eq. (59) behaves [9] as

$$\langle \hat{T}_i \hat{T}_{i+r} \rangle \propto \cos\left(\frac{2\pi}{3}r\right). \quad (62)$$

which characterizes a trimer long-range order. Also, in the vicinity of the phase boundary ϕ_c , i.e., $\xi \rightarrow \infty$, these three functions are almost the same.

Recently, controllable quantum many-body systems have been realised in ultracold atoms in an optical lattice. We also believe that our numerical results can be applied to experiments and quantum simulations in such systems. Especially, quantum many-body systems have $SU(\nu)$ (ν : integer) symmetry in ultracold strontium (^{87}Sr) atoms [12] and ytterbium (^{173}Yb) atoms [14] in an optical lattice. These atomic systems are expected to be applied to quantum information processing. Our results will be a part of a basic theory in realising quantum information processing.

ACKNOWLEDGEMENTS

We are grateful to S. Moriya for constructing a useful algorithm, which we modify for our numerical calculations.

A $SU(3)$ AND ITS REPRESENTATION

In this section, we review $SU(3)$ and the representation of $SU(3)$ on the basis of the paper [11] and the book [36], corresponding to the trimer state.

A.1 Gell-Mann matrices

The Gell-Mann matrices, the basis of $SU(3)$ group, are defined as

$$\lambda^1 = \begin{pmatrix} 0 & 1 & 0 \\ 1 & 0 & 0 \\ 0 & 0 & 0 \end{pmatrix}, \lambda^2 = \begin{pmatrix} 0 & -i & 0 \\ i & 0 & 0 \\ 0 & 0 & 0 \end{pmatrix}, \lambda^3 = \begin{pmatrix} 1 & 0 & 0 \\ 0 & -1 & 0 \\ 0 & 0 & 0 \end{pmatrix},$$

$$\lambda^4 = \begin{pmatrix} 0 & 0 & 1 \\ 0 & 0 & 0 \\ 1 & 0 & 0 \end{pmatrix}, \lambda^5 = \begin{pmatrix} 0 & 0 & -i \\ 0 & 0 & 0 \\ i & 0 & 0 \end{pmatrix}, \lambda^6 = \begin{pmatrix} 0 & 0 & 0 \\ 0 & 0 & 1 \\ 0 & 1 & 0 \end{pmatrix},$$

$$\lambda^7 = \begin{pmatrix} 0 & 0 & 0 \\ 0 & 0 & -i \\ 0 & i & 0 \end{pmatrix}, \lambda^8 = \frac{1}{\sqrt{3}} \begin{pmatrix} 1 & 0 & 0 \\ 0 & 1 & 0 \\ 0 & 0 & -2 \end{pmatrix}.$$

They satisfy the commutation relations $[\lambda^a, \lambda^b] = 2f^{abc}\lambda^c$ and are normalized as $\text{tr}(\lambda^a\lambda^b) = 2\delta_{ab}$. The structure constants f^{abc} are totally antisymmetric and the non-vanishing values are given by $f^{123} = i$, $f^{147} = f^{246} = f^{257} = f^{345} = -f^{156} = -f^{367} = i/2$, $f^{458} = f^{678} = i\sqrt{3}/2$.

A.2 Representation of $SU(3)$

Generators \hat{J}^a , Eq. (7), satisfy the algebra

$$[\hat{J}^a, \hat{J}^b] = f^{abc}\hat{J}^c. \quad (63)$$

For the group $SU(3)$, there are two diagonal generators \hat{J}^3 and \hat{J}^8 . Also, the other generators define the ladder operators as

$$\hat{I}^\pm \equiv \hat{J}^1 \pm i\hat{J}^2, \\ \hat{U}^\pm \equiv \hat{J}^6 \pm i\hat{J}^7, \\ \hat{V}^\pm \equiv \hat{J}^4 \pm i\hat{J}^5,$$

respectively. The algebra Eq. (63) is realized by the \hat{J}^a 's, which gives the fundamental representation $\mathbf{3}$ of $SU(3)$ illustrated in Fig. 12. The weight diagram in Fig. 12 instructs us about the eigenvalues of the diagonal generators as well as the actions of the ladder operators of the basis states. Here, we put $|b\rangle \equiv |1\rangle$, $|r\rangle \equiv |0\rangle$, $|g\rangle \equiv |-1\rangle$.

According to Greiter and Rachel [11], a spin-1 \circ , Eq. (12) $\{\circ\circ\}$, and the trimer $\{\circ\circ\circ\}$ are expressed by the representations $\mathbf{3}$, $\bar{\mathbf{3}}$, and $\mathbf{1}$ respectively. The fundamental representation $\bar{\mathbf{3}}$ is also illustrated in Fig. 12, where we define

$$|m\rangle \equiv \frac{1}{\sqrt{2}}(|1, 0\rangle - |0, 1\rangle), \quad (64)$$

$$|c\rangle \equiv \frac{1}{\sqrt{2}}(|1, -1\rangle - |-1, 1\rangle), \quad (65)$$

$$|y\rangle \equiv \frac{1}{\sqrt{2}}(|0, -1\rangle - |-1, 0\rangle). \quad (66)$$

Also, the trimer states on four sites in Eq. (11) can be expressed as

$$\{\circ\circ\circ\} \circ \doteq \mathbf{1} \otimes \mathbf{3} = \mathbf{3}, \quad (67)$$

$$\{\circ\circ\}\{\circ\circ\} \doteq \bar{\mathbf{3}} \otimes \bar{\mathbf{3}} = \mathbf{3} \oplus \bar{\mathbf{6}}, \quad (68)$$

where the weight diagram of $\bar{\mathbf{6}}$ is depicted in Fig. 13

B RENORMALIZATION-GROUP EQUATION

In this section, we review the RG calculation by Itoi and Kato [19] to investigate the critical behaviour around the transition point $\phi = \phi_c$ in this paper.

First of all, we let x_0 denote the time in the system and x_1 be the position of the field. We then define z and \bar{z} as

$$z \equiv x_0 + ix_1, \quad \bar{z} \equiv x_0 - ix_1. \quad (69)$$

We define the action $\hat{\mathcal{A}}$ as

$$\hat{\mathcal{A}} \equiv \hat{\mathcal{A}}_{SU(3)_1} + g_1 \int \frac{d^2z}{2\pi} \hat{\Phi}^{(1)}(z, \bar{z}), \quad (70)$$

where $\hat{\mathcal{A}}_{SU(3)_1}$ is the action of the free fields in the $SU(3)_1$ WZW model [15–17]. $\hat{\Phi}^{(1)}$ is an operator of the marginal field with $SU(3)$ symmetry and chiral \mathbb{Z}_3 symmetry. The scaling variable g_1 is a perturbational parameter. The system remains $SU(3)$ symmetric regardless of the value of g_1 . According to Itoi and Kato [19], the renormalization-group equation for the scaling variables becomes

$$\frac{dg_1(l)}{dl} = \frac{3}{2\sqrt{2}}g_1^2(l). \quad (71)$$

References

- [1] G. V. Uimin, ONE-DIMENSIONAL PROBLEM FOR $S = 1$ WITH MODIFIED ANTIFERROMAGNETIC HAMILTONIAN, JETP Lett. **12**, 225 (1970).

- [2] C. K. Lai, Lattice gas with nearest-neighbor interaction in one dimension with arbitrary statistics, *J. Math. Phys.* **15**, 1675 (1974).
- [3] B. Sutherland, Model for a multicomponent quantum system, *Phys. Rev. B* **12**, 3795 (1975).
- [4] P. P. Kulish and N. Yu. Reshetikhin, Generalized Heisenberg ferromagnet and the Gross-Neveu model, *Sov. Phys. JETP* **53**, 108 (1981).
- [5] Y.-T. Oh, H. Katsura, H.-Y. Lee, and J. H. Han, Proposal of a spin-one chain model with competing dimer and trimer interactions, *Phys. Rev. B* **96**, 165126 (2017).
- [6] T. Mashiko, S. Moriya, and K. Nomura, Universality Class around the SU(3) Symmetric Point of the Dimer–Trimer Spin-1 chain, *J. Phys. Soc. Jpn.* **90**, 024005 (2021).
- [7] I. Affleck, EXACT CRITICAL EXPONENTS FOR QUANTUM SPIN CHAINS, NON-LINEAR σ -MODELS AT $\theta = \pi$ AND THE QUANTUM HALL EFFECT, *Nucl. Phys. B* **265**, 409 (1986).
- [8] I. Affleck, CRITICAL BEHAVIOUR OF SU(n) QUANTUM CHAINS AND TOPOLOGICAL NON-LINEAR σ -MODELS, *Nucl. Phys. B* **305**, 582 (1988).
- [9] A. Schmitt, K.-H. Mütter, M. Karbach, Y. Yu, and G. Müller, Static and dynamic structure factors in the Haldane phase of the bilinear-biquadratic spin-1 chain, *Phys. Rev. B* **58**, 5498 (1998).
- [10] J. Sólyom and J. Zittartz, Exact trimer ground states on a spin-1 chain, *EPL* **50**, 389 (2000).
- [11] M. Greiter and S. Rachel, Valence bond solids for SU(n) spin chains: Exact models, spinon confinement, and the Haldane gap, *Phys. Rev. B* **75**, 184441 (2007).
- [12] B. J. DeSalvo, M. Yan, P. G. Mickelson, Y. N. Martinez de Escobar, and T. C. Killian, Degenerate Fermi Gas of ^{87}Sr , *Phys. Rev. Lett.* **105**, 030402 (2010).
- [13] A. V. Gorshkov, M. Hermele, V. Gurarie, C. Xu, P. S. Julienne, J. Ye, P. Zoller, E. Demler, M. D. Lukin, and A. M. Rey, *Nat. Phys.* **6**, 289 (2010).
- [14] S. Taie, R. Yamazaki, S. Sugawa, and Y. Takahashi, An SU(6) Mott insulator of an atomic Fermi gas realized by large-spin Pomeranchuk cooling, *Nat. Phys.* **8**, 825 (2012).
- [15] J. Wess and B. Zumino, CONSEQUENCES OF ANOMALOUS WARD IDENTITIES, *Phys. Lett. B* **37**, 95 (1971).
- [16] E. Witten, GLOBAL ASPECTS OF CURRENT ALGEBRA, *Nucl. Phys. B* **223**, 422 (1983).
- [17] E. Witten, Non-Abelian Bosonization in Two Dimensions, *Commun. Math. Phys.* **92**, 455 (1984).
- [18] V. G. Knizhnik and A. B. Zamolodchikov, CURRENT ALGEBRA AND WESS-ZUMINO MODEL IN TWO DIMENSIONS, *Nucl. Phys. B* **247**, 83 (1984).
- [19] C. Itoi and M.-H. Kato, Extended massless phase and the Haldane phase in a spin-1 isotropic antiferromagnetic chain, *Phys. Rev. B* **55**, 8295 (1997).
- [20] K. Nomura and S. Takada, A New Phase of the $S = 1$ Bilinear-Biquadratic Chain: –a Trimerized State–, *J. Phys. Soc. Jpn.* **60**, 389 (1991).
- [21] Y. Xian, Spontaneous trimerization of spin-1 chains, *J. Phys. Condens. Matter* **5**, 7489 (1993).
- [22] C. K. Majumdar and D. K. Ghosh, On Next-Nearest-Neighbor Interaction in Linear Chain. I, *J. Math. Phys.* **10**, 1388 (1969).
- [23] J. L. Cardy, Logarithmic corrections to finite-size scaling in strips, *J. Phys. A: Math. Gen.* **19**, L1093 (1986).
- [24] J. L. Cardy, OPERATOR CONTENT OF TWO-DIMENSIONAL CONFORMALLY INVARIANT THEORIES, *Nucl. Phys. B* **270** [FS16], 186 (1986).
- [25] J. L. Cardy, Conformal invariance and universality in finite-size scaling, *J. Phys. A: Math. Gen.* **17**, L385 (1984).
- [26] P. Reinicke, Analytical and non-analytical corrections to finite-size scaling, *J. Phys. A: Math. Gen.* **20**, 5325 (1987).
- [27] A. Kitazawa and K. Nomura, Critical Properties of $S = 1$ Bond-Alternating XXZ Chains and Hidden $\mathbb{Z}_2 \times \mathbb{Z}_2$ Symmetry, *J. Phys. Soc. Jpn.* **66**, 3944 (1997).
- [28] H. W. J. Blöte, J. L. Cardy, and M. P. Nightingale, Conformal Invariance, the Central Charge, and Universal Finite-Size Amplitudes at Criticality, *Phys. Rev. Lett.* **56**, 742 (1986).
- [29] I. Affleck, Universal Term in the Free Energy at a Critical Point and the Conformal Anomaly, *Phys. Rev. Lett.* **56**, 746 (1986).
- [30] K. Okamoto and K. Nomura, Fluid–dimer critical point in $S = \frac{1}{2}$ antiferromagnetic Heisenberg chain with next nearest neighbor interactions, *Phys. Lett. A* **169**, 433 (1992).
- [31] A. B. Zamolodchikov, “Irreversibility” of the flux of the renormalization group in a 2D field theory, *JETP Lett.* **43**, 730 (1986).
- [32] N. Chepiga, I. Affleck, and F. Mila, Dimerization transitions in spin-1 chains, *Phys. Rev. B* **93**, 241108(R) (2016).
- [33] N. Chepiga, I. Affleck, and F. Mila, Spontaneous dimerization, critical lines, and short-range correlations in a frustrated spin-1 chain, *Phys. Rev. B* **94**, 205112 (2016).
- [34] E. M. Stoudenmire, S. Trebst, and L. Balents, Quadrupolar corrections and spin freezing in $S = 1$ triangular lattice antiferromagnets, *Phys. Rev. B* **79**, 214436 (2009).
- [35] A. Läuchli, G. Schmid, and S. Trebst, Spin nematics correlations in bilinear-biquadratics $S = 1$ spin chains, *Phys. Rev. B* **74**, 144426 (2006).
- [36] J. F. Cornwell, *Group Theory in Physics* (Academic, London, 1984), Vol. II.

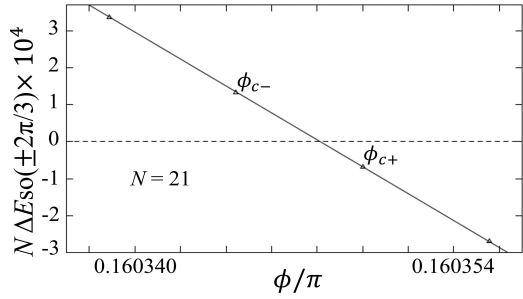
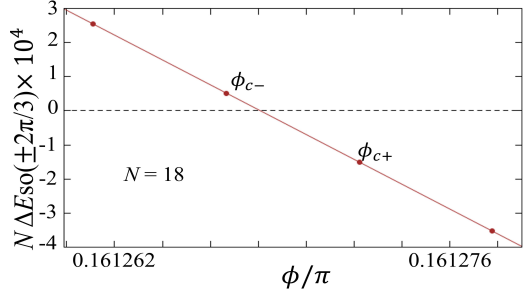
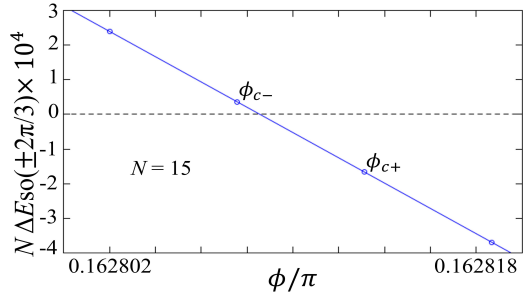


FIG. 6: $N\Delta E_{\text{so}}(\pm 2\pi/3)$ in the vicinity of the phase boundary ϕ_c with $N = 15-21$.

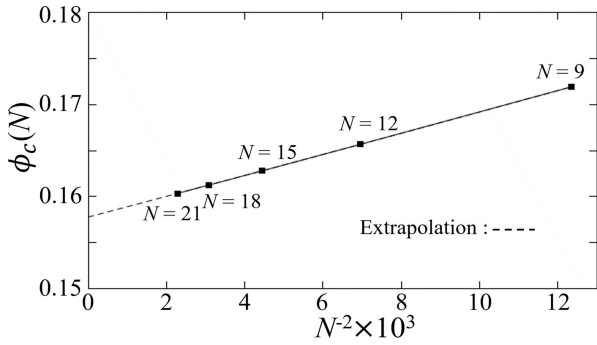


FIG. 7: Phase boundary $\phi_c(N)$ as a function of N^{-2} with $N = 9-21$.

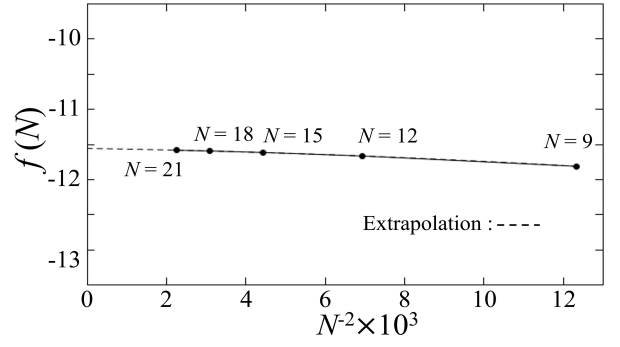


FIG. 8: $f(N)$ as a function of N^{-2} with $N = 9-21$.

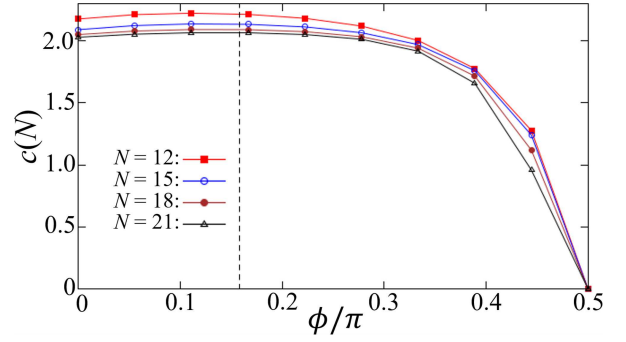


FIG. 9: Effective central charge $c(N)$ as a function of ϕ with $N = 12-21$. The dashed line is $\phi = \phi_c$, where we put $\phi_c = 0.15779\pi$.

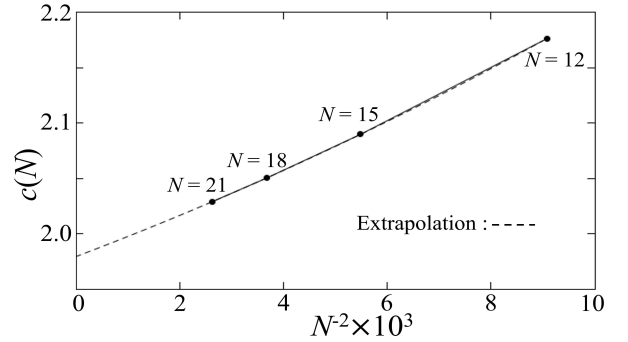


FIG. 10: Effective central charge $c(N)$ with $N = 12-21$ at $\phi = 0$.

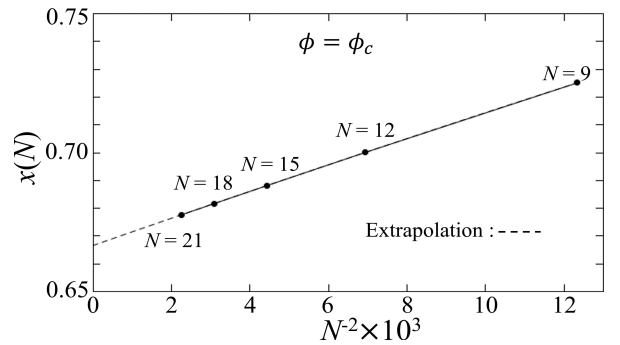


FIG. 11: Effective scaling dimension $x(N)$ with $N = 9-21$ at $\phi = \phi_c$.

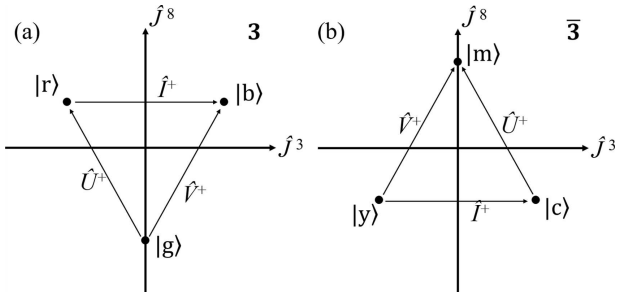


FIG. 12: Weight diagrams of the fundamental representations, (a) $\mathbf{3}$ and (b) $\bar{\mathbf{3}}$.

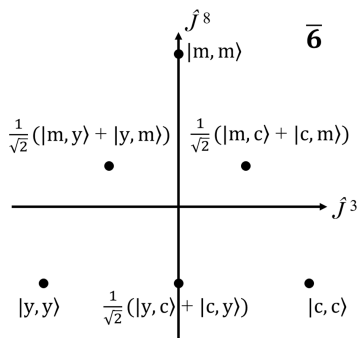


FIG. 13: Weight diagram of the representation $\bar{\mathbf{6}}$.